Electronic Supplementary Material (ESI) for Chemical Communications.

Supporting Information

pH-switchable Pickering miniemulsion enabled by carbon quantum dots for quasi-homogenized biphasic catalytic system

Lin Ni, *Chang Yu*,* *Yuanyang Xie*, *Qianbing Wei*, *Dongming Liu*, *Xinyi Tan*, *Yiwang Ding*, *and Jieshan Qiu**

Table of Contents

Experimental Procedures

Chemical reagents and materials

All chemicals were used directly as received, including toluene (AR, Kermel, CAS# 100−88−3), ethanol (GR, Aladdin, CAS# 64−17−5), sodium hydroxide (AR, Kermel, CAS# 1310−73−2), citric acid (GR, Aladdin, CAS# 5949−29−1), sodium borohydride (AR, Aladdin, CAS# 16940−66−2), hydrogen peroxide (30 wt%, Kermel, CAS# 7722−84−1), cyclohexane (AR, Kermel, CAS# 110−82−7), styrene (AR, Kermel, CAS# 100−42−5), dichloromethane (AR, Kermel, CAS# 75−09−2), nitrobenzene (GC, Aladdin, CAS# 98−95−3), decalin (GR, Ourchem, CAS# 91−17−8), benzyl alcohol (AR, Aladdin, CAS# 1000−51−6), benzaldehyde (AR, Aladdin, CAS# 100−52−7) hydrochloric acid (AR, Kermel, CAS# 7647−01−0), octadecylamine (GC, Aladdin, CAS# 124−30−1), ethyl acetate (99%, Kermel, CAS# 141−78−6), graphite (99.95%, 750−850 mesh, Aladdin, CAS# 7782−42−5). Graphene oxide (GO) was obtained by the modified Hummers method.[1]

Catalyst synthesis and Characterization

Synthesis of CQDs-$C_{18}N$

The amphiphilic carbon quantum dots were synthesized via the "bottom-up" approach. For a typical procedure, 2 g of citric acid and 1 g of octadecylamine was added into 25 mL of ethonal. The mixture was stirred for 1 h, and the sediment was filtrated and washed with ethonal for three times. The solid powder was dryed at 65 ^{o}C for 24 h, and was heated at 200 ^{o}C in air for 1 h until the white powder was liquated to orange fluid. Then, the liquid was dispersed into the 100 mL of 0.25 M NaOH aqueous solution

dropwise, and stirred (500 rpm) at 40 °C for 36 h. The obtained dispersion was centrifuged at 9000 rpm for 5 min to remove the large impurities, and the small molecules were removed via dialysis (500DA dialysis membrane) for 48 h to obtain the yellow carbon quantum dot solution. The hydrophilic CQDs was obtained followed the same procedure without octadecylamine.[2]

Synthesis of catalysts

The supports and $PdCl_2$ with the mass ratio of 9:1 was added into 25 mL of the water and ethanol mixture (volume ratio of 1:4), and stirred for 4 h. After standing for 12 h, 10 mL of $NaBH_4$ solution (2 mg mL^{-1}, water: ethanol=1:1) was added into the mixture dropwise with constant stirring. The solution was stirred for 1 h for Pd^{2+} reduction, then was centrifuged at 20000 rpm for 20 min. The obtained solid catalyst was washed with deionized water for three times.

Preparation of reversible Pickering miniemulsion

In a typical procedure, the carbon quantum dot solution (0.1 wt%) of 4 mL and oil phase of 2 mL were added into a vial, followed by ultrasound treatment (300 W) for 0.5 min. Then, the mixture went through the mild emulsification process (hand shaking) to form the stable coarse emulsions. Finally, the mixture was homogenized by stirring at 1000 rpm for 10 min to form the stable emulsion.

The pH-responsive Pickering miniemulsion was tested by adding HCl and NaOH solution (1 M) to adjust the pH value. For a typical run, the several drops of HCl solution (1 M) were added into the as-formed emulsion to change the pH value to 3–4, and the emulsion was broken for minutes. After adding several drops of NaOH solution

(1 M) to tune the pH value to 10–11, the emulsion was regenerated by stirring.

Interfacial catalysis reaction

The conversion of the substrates was calculated as follows:

$$Conv. = (C_0 - C) / C_0 \quad (1)$$

Where C_0 represented the initial concentration of the reactants, and C was the concentration of the reactants after reaction.

The selectivity toward the products was calculated as:

$$Sel. = C_p / (C_0 - C) \quad (2)$$

Where C_p was the concentration of the products.

The turnover frequency (*TOF*) value was defined as:

$$TOF = n / (n_{Pd} \times t) \quad (3)$$

Where n denoted the mole of reactants converted, and n_{Pd} represented the mole of Pd in catalysts, which was determined by ICP-OES results. t referred to the reaction time.

Typical procedure of the biphasic oxidation of BA with H_2O_2

10 mg of catalysts were dispersed in 10 mL of 2.2 wt% H_2O_2 aqueous solution, and 5 mL of toluene was used as oil phase. The mixture was treated with ultrasound for 0.5 min, and was homogenized by stirring for 10 min to form the emulsion. Then, the system was heated to the operating temperature, and 2 mmol of BA was added subsequently to trigger the reaction. After different reaction time, the reaction liquor was collected via a filter (0.22 μm), and analyzed by Gas chromatography with flame ionization detector (FID) using a capillary column (SE-54, 30 m × 0.32 mm × 0.6 μm).

Typical procedure of the catalyst recycling

Before reaction, 10 mg of catalysts were dispersed in 10 mL of 2.2 wt% H_2O_2 aqueous solution, and 5 mL of toluene was used as oil phase. The Pickering miniemulsion was formed after the pH value was adjusted to 10−11 by adding NaOH (1 M) followed with the subsequent ultrasound treatment and stirring. Then, the system was heated to the operating temperature, and 2 mmol of BA was added subsequently to trigger the reaction. At the end of the reaction, the emulsion was broken for minutes after adding a few drops of HCl (1 M). The benzaldehyde products in oil phase were resolved in the upper layer, and the catalysts were re-dispersed in aqueous phase after turning the system to neutral conditions by adding NaOH (1 M). The products in oil phase were recovered via liquid separation and catalysts in aqueous phase could be recycled for the next run. To measure the recycling performance for the Pd/CQDs-C_{18}N, 2 mmol of BA in oil phase and H_2O_2 were re-added into the system. The pH value was re-adjusted to 10−11 by adding NaOH (1 M) for the stabilization of Pickering miniemulsion, and the reaction system was heated to the operating temperature to initiate the next interfacial reaction. At the fifth reaction cycle, the catalysts were recovered by centrifugation at 20000 rpm for 20 min, and the bottom layer of water was replaced with equal volume of fresh water for the following cycles.

Typical procedure of the biphasic reduction for the styrene

2 mmol of substrates were dispersed in 5 mL of toluene as oil phase, and 10 mg of catalysts were dispersed in 10 mL aqueous solution. The mixture was treated with ultrasound for 0.5 min, and was homogenized by stirring for 10 min to form the emulsion. Then, 4 mmol of $NaBH_4$ was added into the reaction system to trigger the

reaction at RT with stirring (500 rpm). After different reaction time, the reaction liquor was collected via a filter (0.22 μm), and analyzed by Gas chromatography with flame ionization detector (FID) using a capillary column (SE-54, 30 m × 0.32 mm × 0.6 μm).

Typical procedure of the hydrogenation for nitrobenzene

2 mmol of substrates were dispersed in 5 mL of toluene as oil phase, and 10 mg of catalysts were dispersed in 10 mL aqueous solution. The mixture was treated with ultrasound for 0.5 min, and was homogenized by stirring for 10 min to form the emulsion. Afterwards, the as-formed emulsion was sealed into a 50 mL autoclave (WATTCAS, with in-situ sampling model), and flushed with H_2 three times to remove the air. Then, the autoclave was charged with H_2 to a pressure of 1 MPa, and was heated to 85 ^oC with stirring (500 rpm). After different reaction time, the reaction liquor was collected via a filter (0.22 μm), and analyzed by Gas chromatography with flame ionization detector (FID) using a capillary column (SE-54, 30 m × 0.32 mm × 0.6 μm).

Computation method

The finite-element analysis was performed by commercial software COMSOL Multiphysics 5.6 (Burlington, MA, USA). The model of emulsion droplet with a size of 1 μm for miniemulsion and 100 μm for conventional Pickering emulsion as consistent with the experimental measurement (Fig. S7, S8 and S21c–d) was constructed. The O/W type of emulsion droplet was considered as being the sphere with organic phase (toluene) containing reactant (BA) inside. The reaction was set to be

occurred on the surface of the droplet, and BA was diffused to the droplet surface via convection. The 'Transport of Diluted Species' model was conducted in time-dependent mode in three dimensions, and the default equations in the COMSOL Multiphysics 5.6 were used. For the mass transfer within the droplet by convection, the Fick's second law was shown as:

$$\frac{\partial C}{\partial t} = D\nabla^2 C \tag{4}$$

Where, C represented the concentration of the reactant; D was the diffusion coefficient of the reactant; t referred to the reaction time. The D value of BA in toluene was set to be 3.71×10^{-9} m^2 s^{-1}. The oxidation of BA followed the first-order reaction and the rate constant was obtained according to the experimental results.

Characterization

The morphology of the catalyst was examined by Transmission electron microscopy (TEM), High angle annular dark field scanning transmission electron microscopy (HAADF-STEM) and High-resolution Transmission electron microscopy (HRTEM). TEM images were taken on HT7700 EXALENS. HAADF-STEM and HRTEM were conducted on FEI Tecnai G2 F30. The thickness of the materials was tested on Dimension ICON atomic force microscope (AFM) in ScanAsyst model. The Fourier transform infrared (FT-IR) spectra were recorded on a Bruker INVENIO R spectrometer (KBr pellet technique). Ultraviolet-visible adsorption spectra were tested by Ultraviolet-visible (UV-Vis) spectrophotometer (Lambda 750S). Emission spectra of the CQDs-C_{18}N with different wavelengths were recorded on Hitachi F7000. ICP-OES was carried out on PerkinElmer Optima 2000DV. X-ray photoelectron spectroscopy (XPS) test was carried out on Thermo ESCALAB 250 using a single Al-K-X-ray source operating at 300 W and 15 kV. Dynamic light scattering (DLS) and

Zeta potential were performed on Malvern ZS90.

The contact angles were measured using a KINO SL150E instrument with high-speed camera. Before measurement, the carbon quantum dot solution was dripped onto quartz plate and dried at 80 ^{o}C overnight for testing. The emulsion droplet was monitored by confocal microscopy in a LabRAM HR Evolution Raman spectrometer. To enhance the visibility, a drop of emulsion was added on the mirror and covered with the coverslip. The well-focused microscopic images of the submicron-sized droplet were difficult to obtain by optical microscope. Therefore, the dried emulsion was observed by FE-SEM. Several drops of emulsion were dispersed on a silicon wafer (1 cm × 1 cm), then moved inside a vacuum drying oven at 25 ^{o}C for drying. The silicon wafer with drying sample was fixed on the specimen stage of the SEM instrument (HITACHI UHR FE-SEM SU8220) by conductive adhesive. Then, the sample was sputter coated with gold for testing. For identification of the emulsion type, the lipophilic Nile red was dissolved in toluene, then a drop of emulsion was added to the system. If the emulsion and red droplet were combined, the water-in-oil type was formed. If not, the oil-in-water type was formed.

Results and Discussion

Additional Supplementary Figures

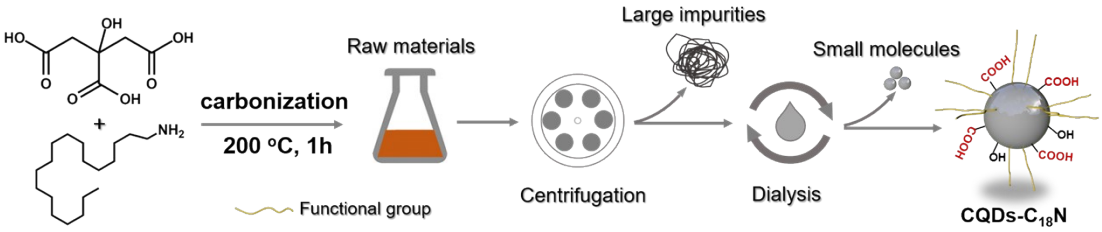

Fig. S1 Scheme illustration of the synthetic procedure for CQDs-C_{18}N.

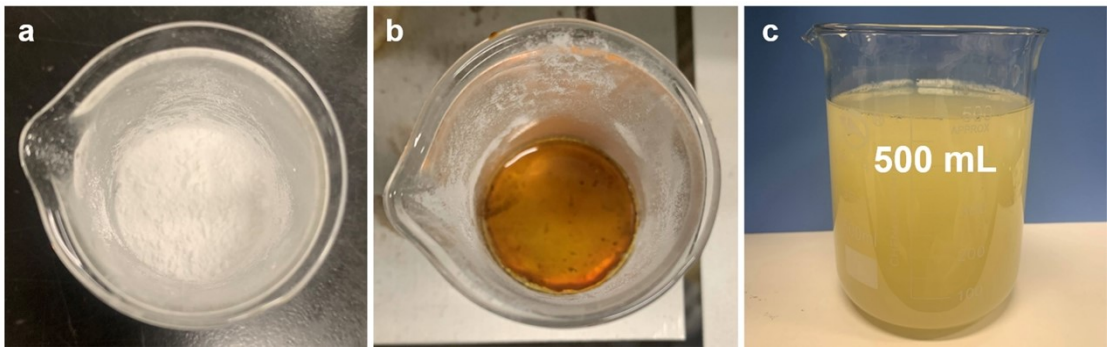

Fig. S2 Optical images of (a) raw materials of the citric acid and octadecylamine, b) the orange fluid after thermal carbonization, and (c) the CQDs-C_{18}N solution.

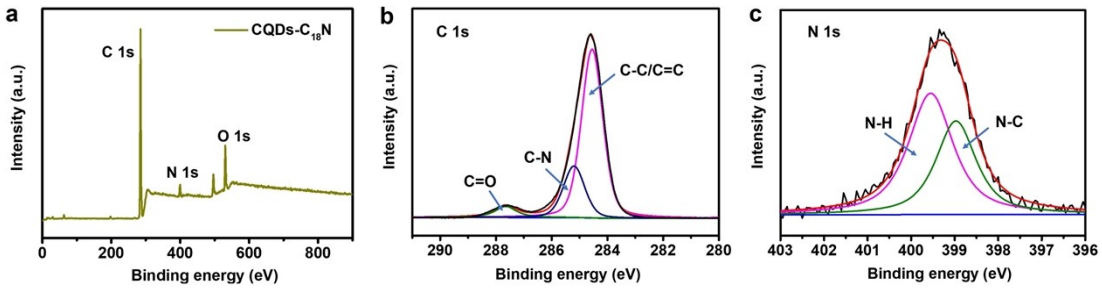

Fig. S3 (a) XPS survey spectrum, high-resolution (b) C 1s and (c) N 1s spectra of CQDs-C_{18}N.

The survey XPS spectrum indicated the presence of C, N and O on the surface of CQDs-C_{18}N (Fig. S3a). The C 1s spectrum was deconvoluted into three peaks at 284.6, 285.2 and 287.6 eV which were assigned to the sp^2 C–C, the amide C–N and oxygen-rich C=O groups, respectively (Fig. S3b).[3] The high-resolution N 1s spectrum was consisted of two peaks at 398.9 and 399.6 eV, which were assigned to C–N and N–H groups, respectively, further confirming the existence of amide group (Fig. S3c) and being in good agreement with FT-IR results.

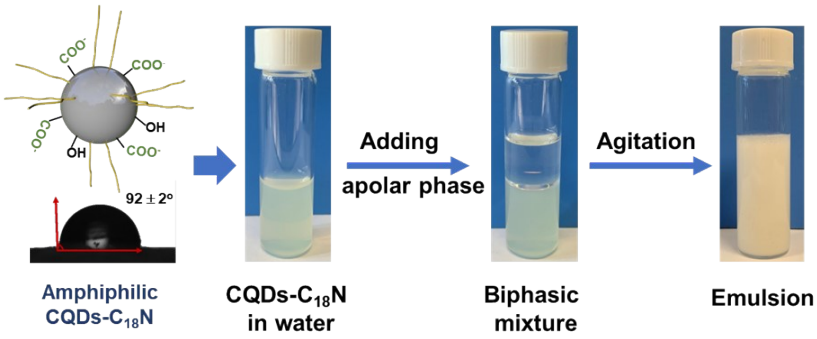

Fig. S4 The emulsification process for the mixture of water and toluene with a volume ratio of 2:1 stabilized by amphiphilic CQDs-C_{18}N (0.1 wt%). The biphasic mixture of water and toluene was taken as a model system to evaluate the emulsion states.

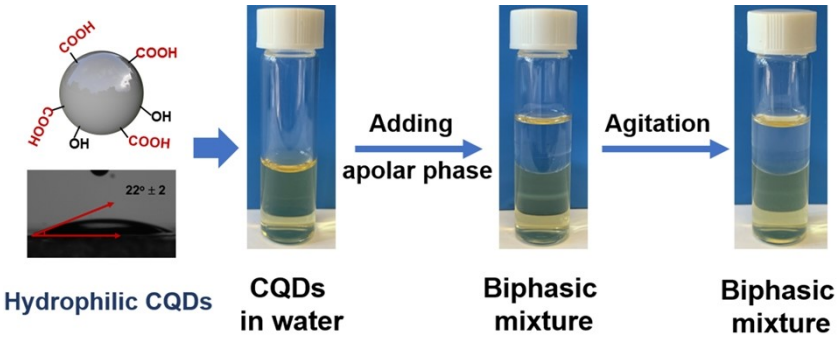

Fig. S5 The emulsification process for the mixture of water and toluene with a volume ratio of 2:1 stabilized by hydrophilic CQDs (0.1 wt%).

There was no Pickering emulsion observed for the unmodified hydrophilic carbon quantum dots (CQDs), and overwhelmingly hydrophilic CQDs preferred to disperse in the lower aqueous phase. The unmodified hydrophilic CQDs were prepared with the same procedures as CQDs-$C_{18}N$ without adding octadecylamine.

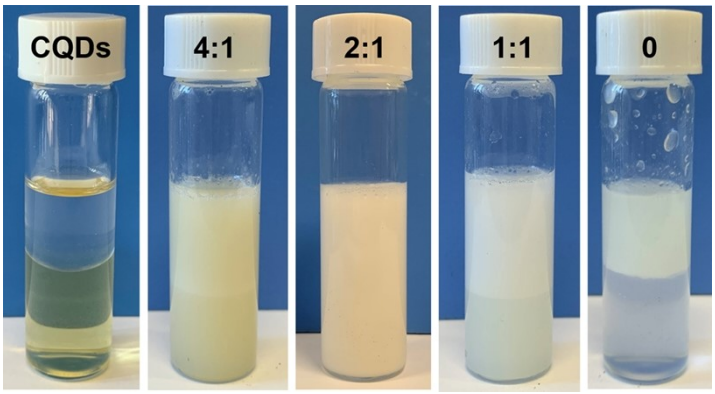

Fig. S6 The emulsion properties of the carbon quantum dot with the different mass ratios of two reactants (citric acid to octadecylamine). To obtain the desired interfacial activity, the mass ratio of the two reactants (citric acid and octadecylamine) was adjusted. The amphiphilic CQDs-$C_{18}N$ with the ratio of 2:1 featured an optimal emulsification capability and the corresponding volume fraction of emulsion was 100%, which was used to the further analysis of emulsion behaviour and catalysis. For comparison, the hydrophobic octadecylamine without citric acid was treated with the same procedure and the product dispersed in the upper oil phase while no emulsion was formed after the identical emulsification process.

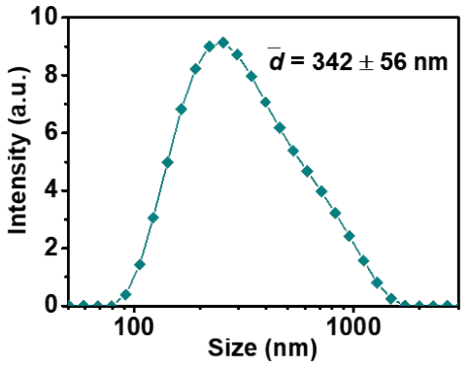

Fig. S7 DLS spectrum of as-formed O/W Pickering miniemulsion.

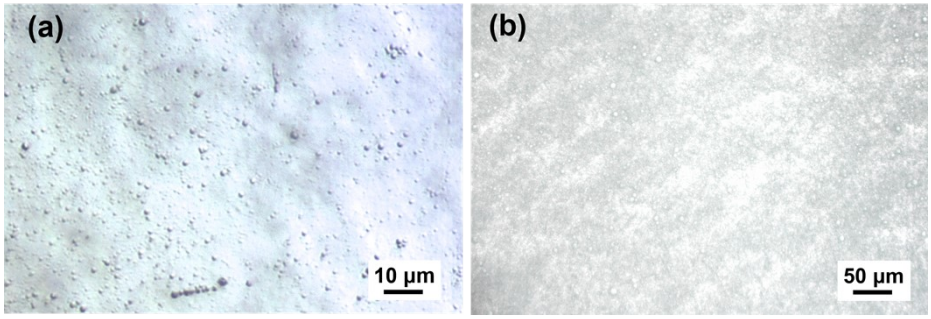

Fig. S8 Optical microscopic images of as-formed O/W miniemulsion formed by CQDs-$C_{18}N$ with (a) high and (b) low magnification. There was no large-sized droplets (10–1000 μm) visible at current state.

Fig. S9 Digital photo of emulsion stabilized by CQDs-$C_{18}N$ in the presence of lipophilic Nile red in toluene, indicative of the formation of oil-in-water emulsion.

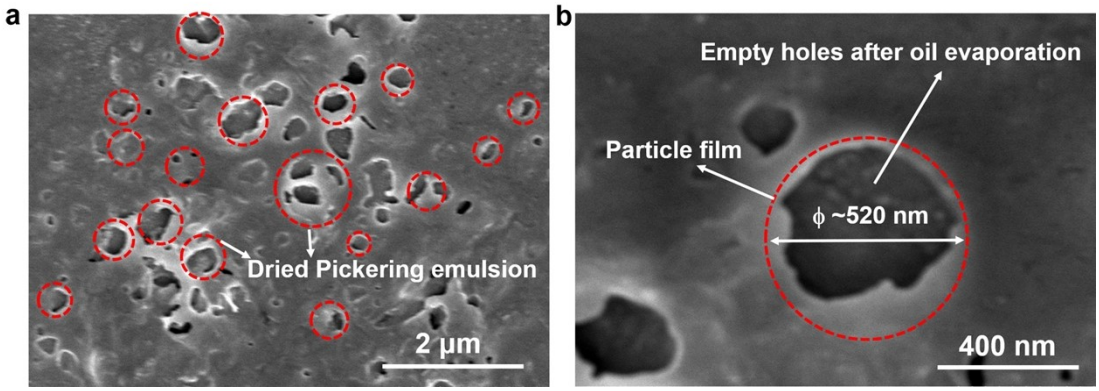

Fig. S10 SEM images of the dried Pickering miniemulsion with (a) low and (b) high magnification.

The spherical empty holes leaved by oil evaporation and the particle film formed by the CQDs-C_{18}N at oil-water interface could be clearly observed, with a size of the dried emulsion below 1 μm.

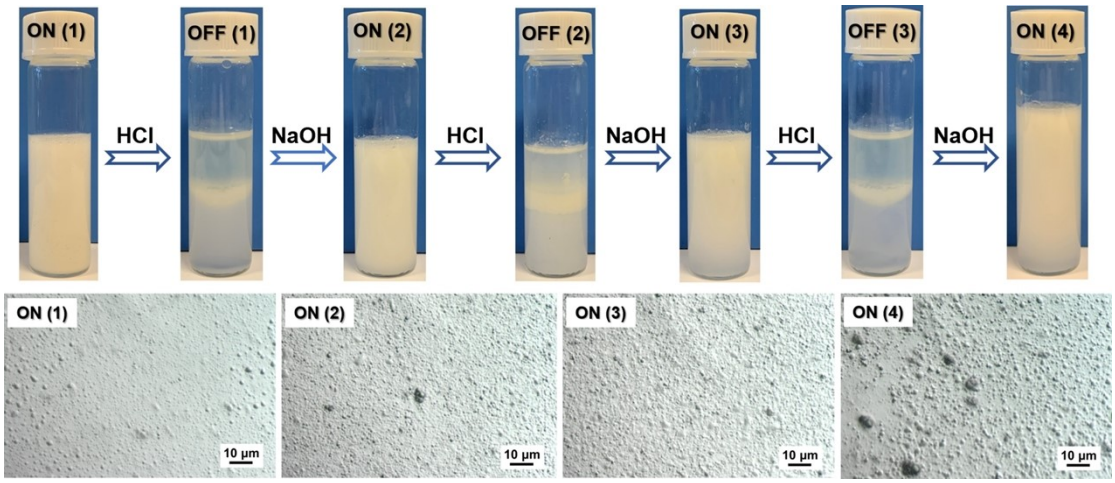

Fig. S11 Digital photos and micrographs of pH-responsive emulsion stabilized by CQDs-C_{18}N (0.1 wt%) during four successive runs.

The volume ratio of water to toluene was 2:1, and HCl (1 M) and NaOH (1 M) solution were used to trigger the emulsification and demulsification/phase separation. Consequently, the as-constructed smart Pickering miniemulsion greatly benefited the green operation of the catalyst recycling and reuse as well as product separation for interfacial catalysis.

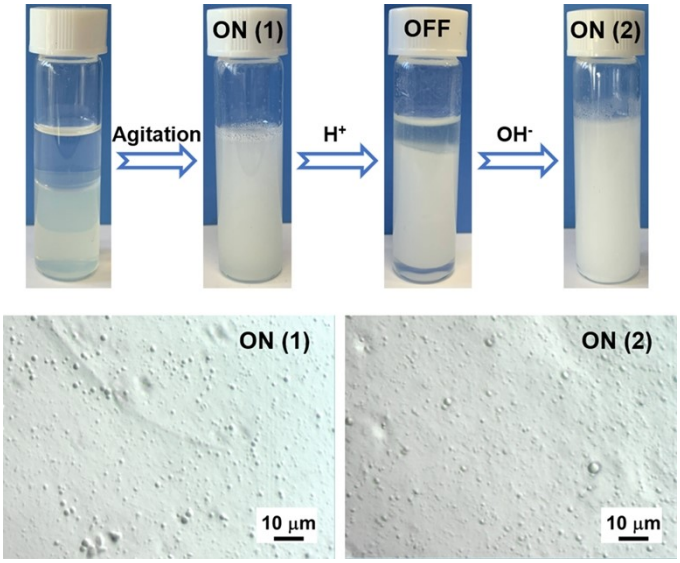

Fig. S12 Digital photos and microscopic images for the successive pH-responsive Pickering miniemulsion stabilized by CQDs-$C_{18}N$ (0.1 wt%) using cyclohexane as oil phase.

The volume ratio of water to cyclohexane was 2:1, and HCl (1 M) and NaOH (1 M) solution were used to trigger the emulsification and demulsification/phase separation.

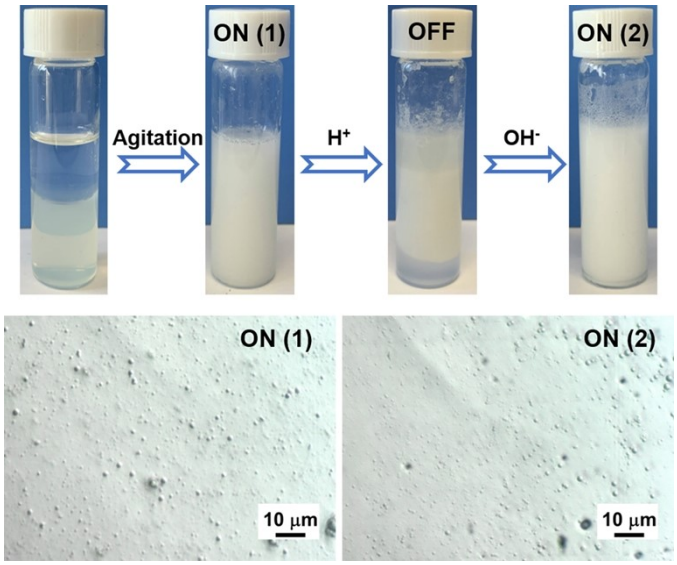

Fig. S13 Digital photos and microscopic images for the successive pH-responsive Pickering miniemulsion stabilized by CQDs-C_{18}N (0.1 wt%) using decalin as oil phase.

The volume ratio of water to decalin was 2:1, and HCl (1 M) and NaOH (1 M) solution were used to trigger the emulsification and demulsification/phase separation.

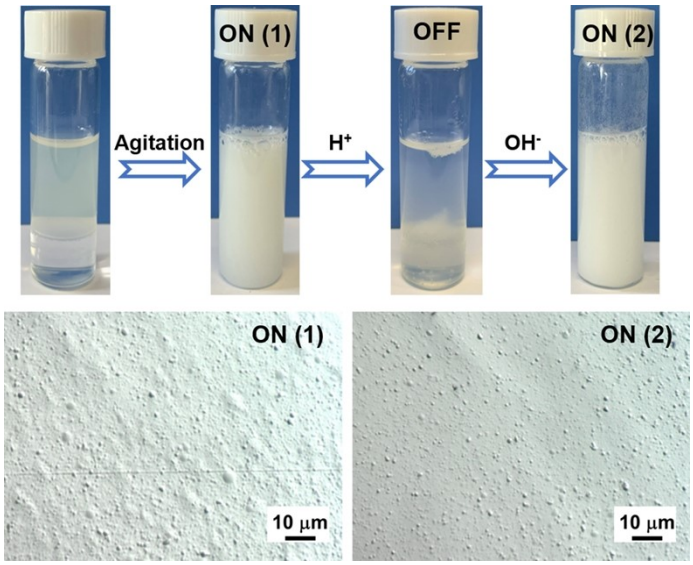

Fig. S14 Digital photos and microscopic images for the successive pH-responsive Pickering miniemulsion stabilized by CQDs-$C_{18}N$ (0.1 wt%) using dichloromethane as oil phase.

The volume ratio of water to dichloromethane was 2:1, and HCl (1 M) and NaOH (1 M) solution were used to trigger the emulsification and demulsification/phase separation.

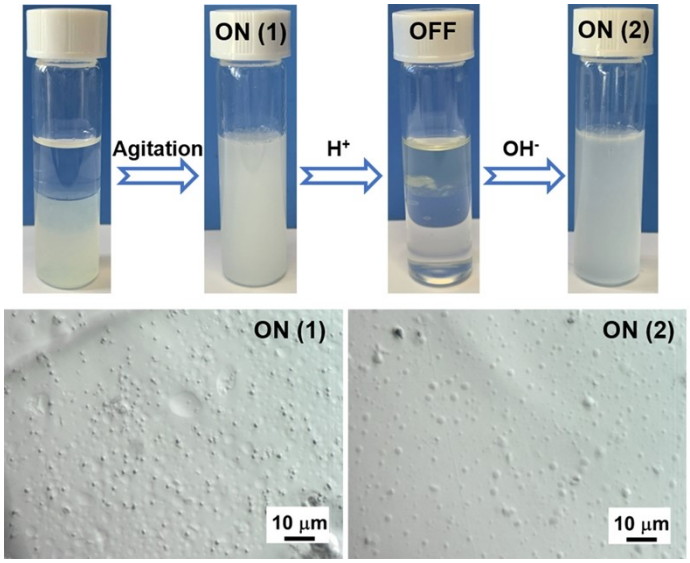

Fig. S15 Digital photos and microscopic images for the successive pH-responsive Pickering miniemulsion stabilized by CQDs-C_{18}N (0.1 wt%) using ethyl acetate as oil phase.

The volume ratio of water to ethyl acetate was 2:1, and HCl (1 M) and NaOH (1 M) solution were used to trigger the emulsification and demulsification/phase separation.

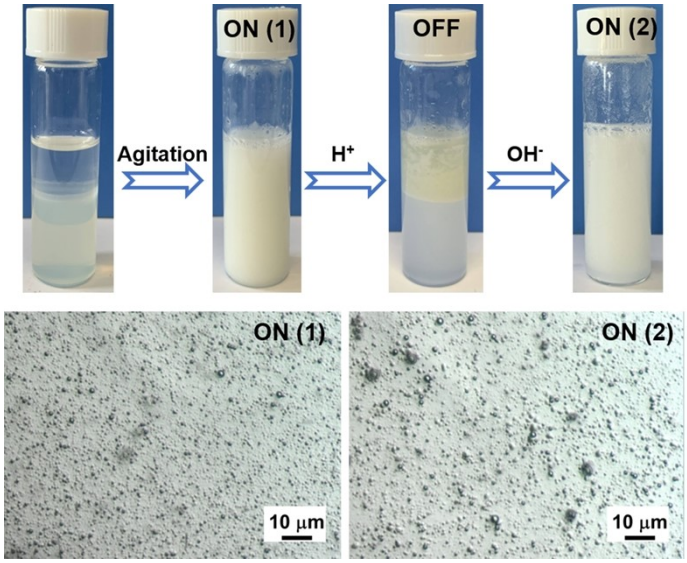

Fig. S16 Digital photos and microscopic images for the successive pH-responsive Pickering miniemulsion stabilized by CQDs-C_{18}N (0.1 wt%) using styrene as oil phase.

The volume ratio of water to styrene was 2:1, and HCl (1M) and NaOH (1M) solution were used to trigger the emulsification and demulsification/phase separation.

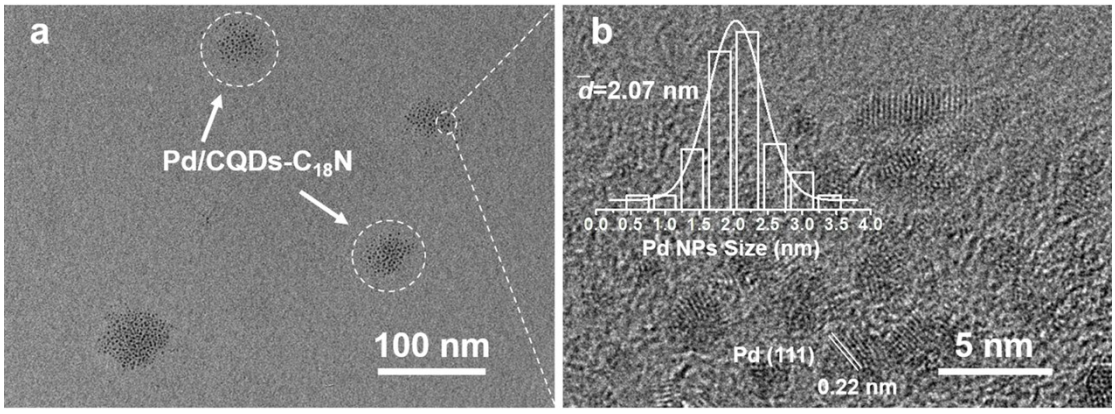

Fig. S17 (a) TEM and (b) HRTEM images of Pd/CQDs-C_{18}N. The Pd/CQDs-C_{18}N was marked by the white circles.

The HRTEM image clearly identified the defined lattice fringes, as highlighted by white lines, with an interplanar spacing of 0.22 nm, which are consistent with the (111) crystalline planes of face-centered-cubic (*fcc*) Pd.[5] TEM images revealed that the Pd particles were uniformly distributed on the surface of the CQDs-C_{18}N with a loading of 1.95 wt%.

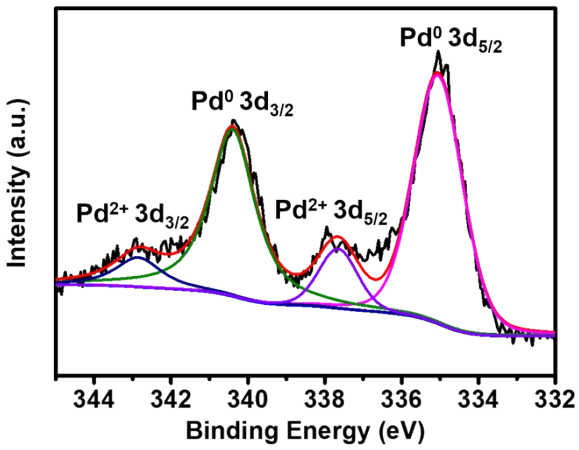

Fig. S18 High-resolution XPS Pd 3d spectrum of Pd/CQDs-$C_{18}N$. The result showed that Pd^0 was the dominant component.

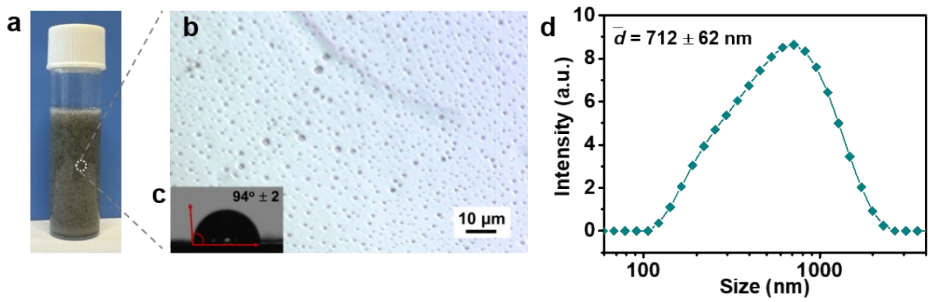

Fig. S19 (a) Digital photo and (b) microscopic image of Pickering miniemulsion stabilized by Pd/CQDs-C_{18}N. (c) The contact angle of Pd/CQDs-C_{18}N. (d) DLS spectrum of as-formed Pickering miniemulsion stabilized by Pd/CQDs-C_{18}N.

After the addition of the oil phase (toluene) to the Pd/CQDs-C_{18}N solution and subsequent emulsification process, the macroscopically quasi-homogeneous Pickering miniemulsion was indeed formed for Pd/CQDs-C_{18}N, as exhibited by the digital photo (Fig. S19a) and the microscopic image (Fig. S19b). Also, the dynamic light scattering (DLS) results of the as-formed Pickering miniemulsion revealed that the size distribution of the droplets was submicron with a mean size of ~712 nm, further revealing that the submicron-sized droplets were successfully stabilized (Fig. S19d).

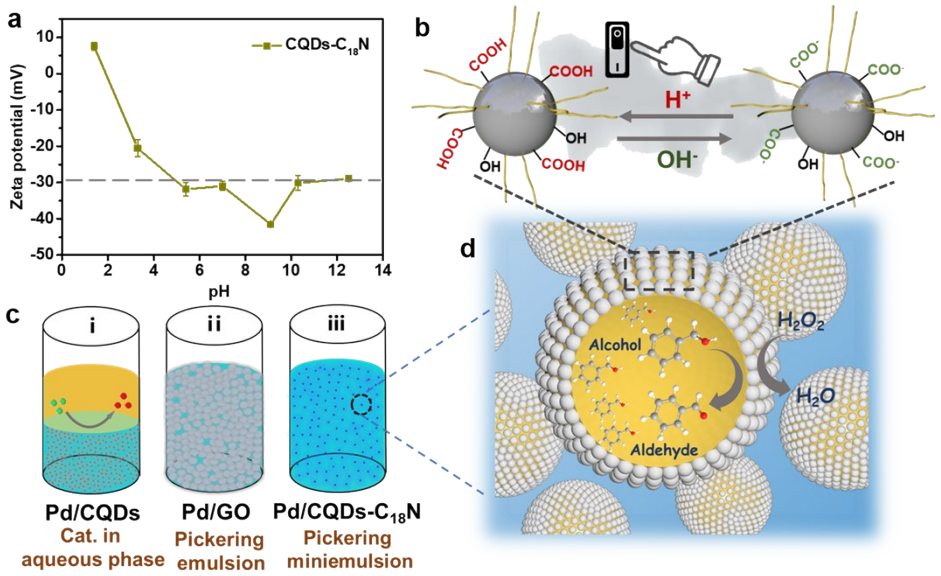

Fig. S20 Smart Pickering miniemulsion induced by pH-responsive CQDs-C_{18}N. (a) Zeta potential of CQDs-C_{18}N (0.1 wt%) dispersed in aqueous solution with different pH values. (b) Structure of pH-responsive CQDs-C_{18}N with acid or base for protonation and deprotonation. (c) Schematic representation of the various reaction systems for the control group experiment. (d) Schematic illustration of BA oxidation in the Pickering miniemulsion system, catalyzed by Pd/CQDs-C_{18}N at the droplet interface.

As for the stable Pickering miniemulsion, the high energy barrier was usually required to break the emulsion for demulsification, because the energy needed for detaching the particle from the liquid/liquid interface was several magnitudes higher than the thermal energy.[4] Fortunately, the amphiphilicity of the smart CQDs-C_{18}N could be controlled by varying the pH values, which changed the ionization degree of the oxygen-rich groups (–COOH) in the CQDs-C_{18}N, and the pH-responsive amphiphilicity of CQDs-C_{18}N gave the opportunities to switch the emulsion behavior. In alkaline solution, the–COOH groups were deprotonated, and the zeta potential was below -30 mV (Fig. S20a), which made the CQDs-C_{18}N more charged and kept electrostatic repulsive interaction in the solution to stabilize the emulsion. When the pH value was decreased

to 6–7, the –COOH groups were partially protonated and the zeta potential was still measured to be about -30 mV, which demonstrated its well water dispersibility under neutral conditions. As the solution was adjusted to be acidic (pH=2), the zeta potential increased to 0–10 mV, indicating the completely protonation of the –COOH and the aggregation of the CQDs-$C_{18}N$ to demulsify the emulsion.

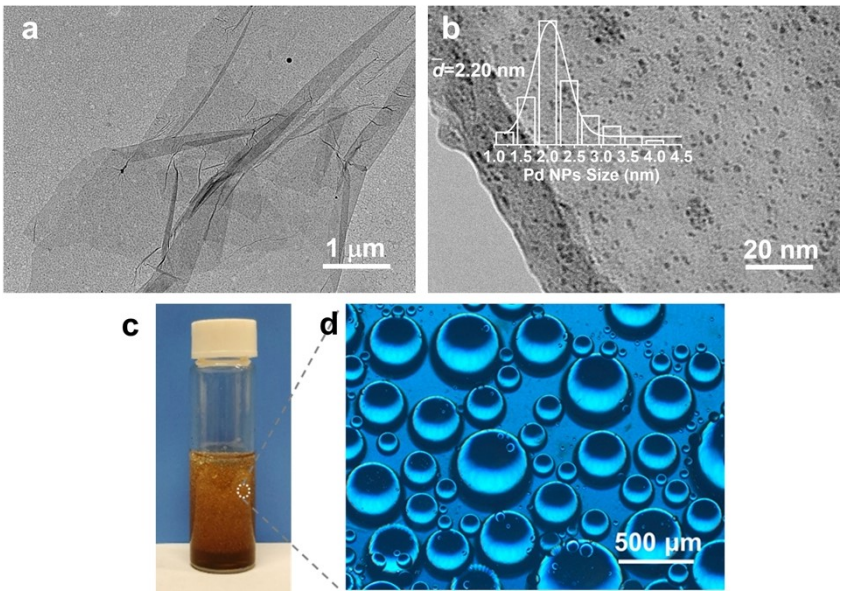

Fig. S21 (a) TEM image of GO with tens of microns in lateral size. (b) TEM image of Pd/GO. (c) Digital photo and (d) microscopic image of Pickering emulsion stabilized by GO.

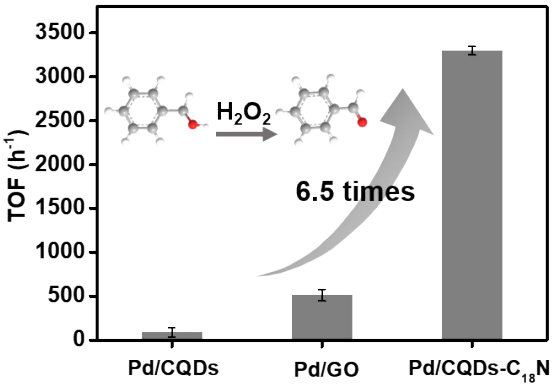

Fig. S22 Variation of turnover frequency (TOF) over different Pd-based catalysts. Inset: chemical structures of the substrate and product; TOF was calculated on the basis of the mole of converted BA (reaction time: 0.25 h) per mole of Pd (determined from ICP-OES results) per hour.

As a proof of concept, the biphasic oxidation of benzyl alcohol (BA) with H_2O_2 was chosen as a model to evaluate the catalytic efficiency and recyclability, because the corresponding carbonyl product is the key intermediate for fine chemical synthesis as well as the avoided use of the toxic inorganic oxidants.[6]

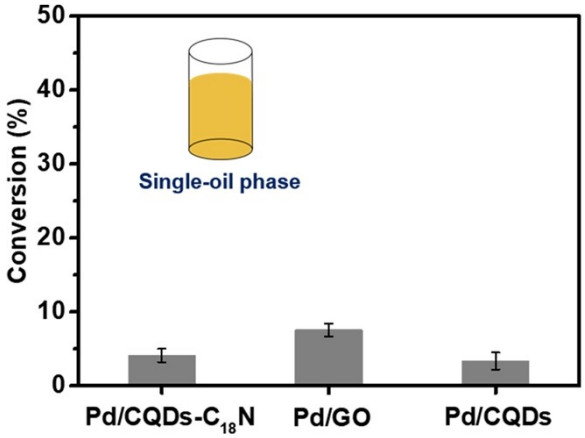

Fig. S23 The conversion of BA over different Pd-based catalysts in single-oil phase. Reaction time: 0.5 h.

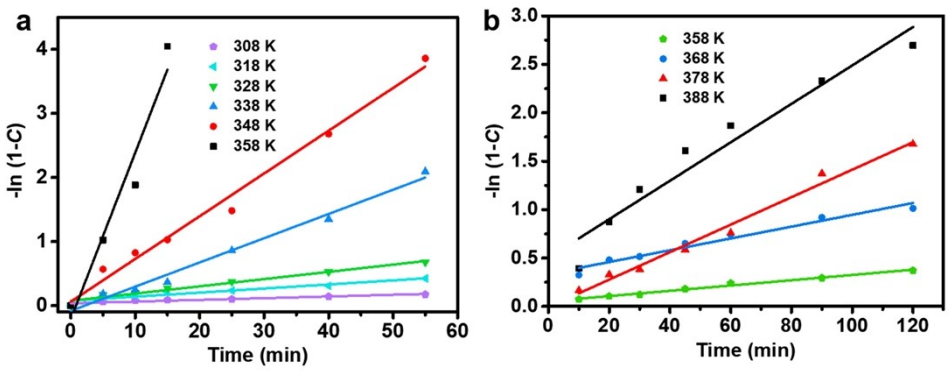

Fig. S24 Kinetic curves of BA oxidation at varied temperatures over Pd/CQDs-$C_{18}N$ in (a) Pickering miniemulsion and (b) single-oil phase system.

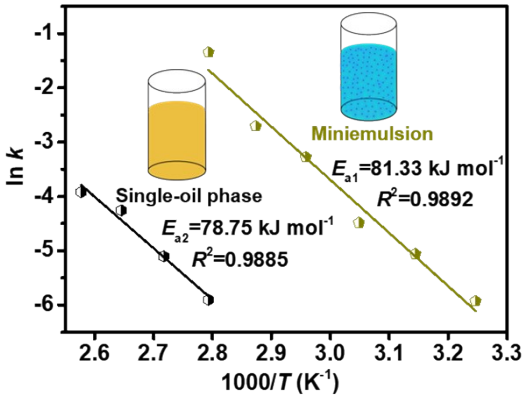

Fig. S25 Catalytic kinetics of BA oxidation over Pd/CQDs-$C_{18}N$ in Pickering miniemulsion and single-oil phase. By plotting the correlation of ln(k) with respect to 1000/T (T denoted the reaction temperature), the E_a was calculated from the slope.

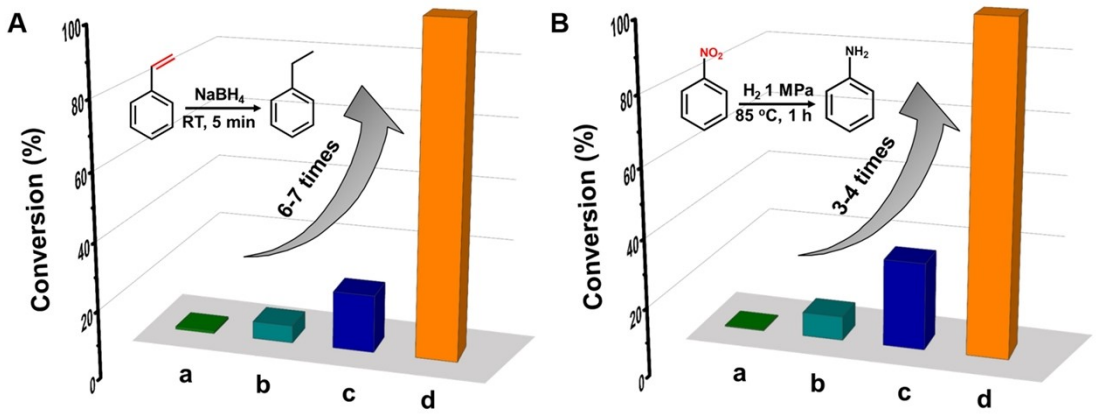

Fig. S26 (A) Catalytic reduction of styrene with $NaBH_4$ to ethylbenzene over various conditions: a. blank experiment without catalysts; b. Pd/CQDs; c. Pd/GO; d. Pd/CQDs-$C_{18}N$. Reaction conditions: 2 mmol substrates, 5 mL toluene as oil phase, 10 mg of 2 wt% Pd-based catalysts dispersed in 10 mL aqueous solution, 4 mmol $NaBH_4$, RT, 5 min of reaction time. (B) Catalytic hydrogenation of nitrobenzene. Reaction conditions: 2 mmol substrates, 5 mL toluene as oil phase, 10 mg of 2 wt% Pd-based catalysts dispersed in 10 mL aqueous solution, 1 MPa H_2, 85 °C, 1 h of reaction time.

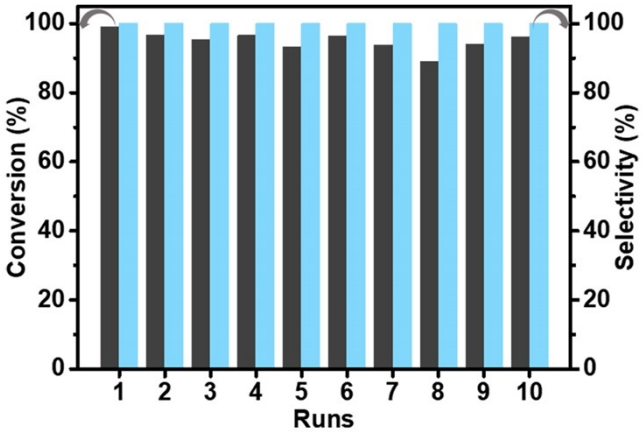

Fig. S27 Recyclability test over Pd/CQDs-$C_{18}N$ in Pickering miniemulsion. Reaction time was 0.5–1 h. Reaction conditions: 2 mmol of BA dissolved in 5 mL of toluene as oil phase, 10 mg of 2 wt% Pd-based catalysts dispersed in 10 mL of 2.2 wt% H_2O_2 aqueous solution, 85 °C.

References

1. W. S. Hummers and R. E. Offeman, *J. Am. Chem. Soc.*, 1958, **80**, 1339; X. Meng, C. Yu, X. Song, J. Iocozzia, J. Hong, M. Rager, H. Jin, S. Wang, L. Huang, J. Qiu and Z. Lin, *Angew. Chem. Int. Ed.*, 2018, **57**, 4682-4686; C. Zhao, C. Yu, B. Qiu, S. Zhou, M. Zhang, H. Huang, B. Wang, J. Zhao, X. Sun and J. Qiu, *Adv. Mater.*, 2018, **30**, 1702486.
2. Y. Dong, J. Shao, C. Chen, H. Li, R. Wang, Y. Chi, X. Lin and G. Chen, *Carbon*, 2012, **50**, 4738-4743.
3. Y. Guo, R. Zhang, S. Zhang, H. Hong, Y. Zhao, Z. Huang, C. Han, H. Li and C. Zhi, *Energy Environ. Sci.*, 2022, **15**, 4167-4174.
4. K. Du, E. Glogowski, T. Emrick, T. P. Russell and A. D. Dinsmore, *Langmuir*, 2010, **26**, 12518-12522; H. Yang, T. Zhou and W. Zhang, *Angew. Chem. Int. Ed.*, 2013, **52**, 7455-7459.
5. W. Zhu, S. Kattel, F. Jiao and J. G. Chen, *Adv. Energy Mater.*, 2019, **9**, 1802840; J. Zhang, B. Wang, E. Nikolla and J. W. Medlin, *Angew. Chem. Int. Ed.*, 2017, **56**, 6594-6598.
6. H. Fan, B. Chen, C. Chen, Z. Zhang, J. Song, G. Yang and B. Han, *Green Chem.*, 2021, **23**, 6341-6348.